Journal of Physics: Conference Series **548** (2014) 012034 doi:10.1088/1742-6596/548/1/012034

Line Shape Measurement and Modelling for Plasma Diagnostics

G Revalde[1], N Zorina[2] and A Skudra[2]

[1]Institute of Technical Physics, Riga Technical University, Āzenes str. 14/24, Riga, Latvia

[1]Ventspils University College, Inženieru str.101, Ventspils, Latvia

[2]Institute of Atomic Physics and Spectroscopy, University of Latvia, Skunu str. 4, Rīga, Latvia, LV 1050

gitar@latnet.lv

Abstract. In this paper we discuss different methods of narrow spectral line shape measurements for a wide spectral range by means of high-resolution spectrometers such as the Fabry-Perot spectrometer, Zeeman spectrometer and Fourier transform spectrometer as well as a theoretical model for spectral line shape modelling and solving of the inverse task based on Tikhonov's regularization method. Special attention is devoted to the line shape measurements for the optically thin light sources filled with Hg, Ar, Xe, Kr for their use in high precision analysers for detection of heavy metals and benzene.

1. Introduction

Line shape diagnostics are essential when light sources with well-defined shapes of the emission lines are required. In this paper we present the spectral line shape measurement and calculation methods created for optimisation needs for special types of low pressure lamps for their application in atomic absorption spectrometers (AAS). Novel type AA analysers are developed for detection of heavy metals, benzene, toluene and other pollutants in air, water and food in real time [1].High selectivity and very low limits of detection depend on the quality of the spectral line shape.

Spectral line shapes are known as important tools for emission plasma diagnostics in different type of plasma since the form of the line is determined by all plasma processes. However many processes act at the same time, and it is not easy to resolve partial effects on the total line shape. In addition, the processes often correlate with each other. We have to take into account also the influence of spectral apparatus. Reconstructing the real line shape from the measured one is a so called inverse ill-posed task since small uncertainties in the measurement give large deviations in solution. Since it is a complex task, sometimes consideration of the instrument function is omitted. It can be done if the width of the instrument function is much smaller than the real spectral line shape which is true in general for high temperatures and dense plasmas. However in the case of low–pressure plasma the instrument function is on the same order as experimental profile and it has to be taken into account.

In this work we will focus on the deconvolution of narrow real spectral line shapes from experimental profiles registered by different spectrometers with high precision. The influence of the

instrument functions on Hg emission lines from low-temperature discharges will be discussed for Fabry-Perot, Zeeman and Fourier transform spectrometers. The influence of the instrument function on the FWHM of spectral line shapes and gas temperature estimation will be elaborated.

2. Experimental details

The developed light sources contain reservoir with working element, capillary and excitation electrodes located outside the capillary and exciting the discharge at 100 MHz frequency. The discharge can be excited also in the bulb of the lamp. Set-up of capillary light source is shown in Fig.1. In this work, experiments were conducted with mercury light sources with different buffer gases Ar, Kr and Xe. To avoid the splitting and consequently the broadening of the spectral line, the isotopes of the metal are used as filling elements.

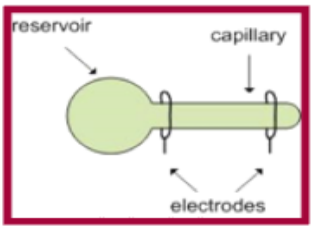

Figure 1. Set-up of a capillary light source

2.1. Fabry-Perot Interferometer

Since the working lines, selected for the needs of AAS, are narrow and often in the UV, the registration instrument should have high sensitivity in broad spectral region. Direct spectral line shape's measurements were done by three different methods in this work. In Fig. 2, the experimental arrangement of a high resolution scanning Fabry-Perot spectrometer is illustrated. The heart of this experimental arrangement is the Fabry-Perot interferometer, consisting of two parallel mirrors, placed into a vacuum chamber which is connected with the pumping system and evacuated. When the air is gradually let to refill the vacuum chamber the refraction index of the mirrors is changing and the spectrum lines are registered by a PMT. The instrument function of the Fabry-Perot interferometer is so called Airy function which can be approximated also by Voigt profile [2].

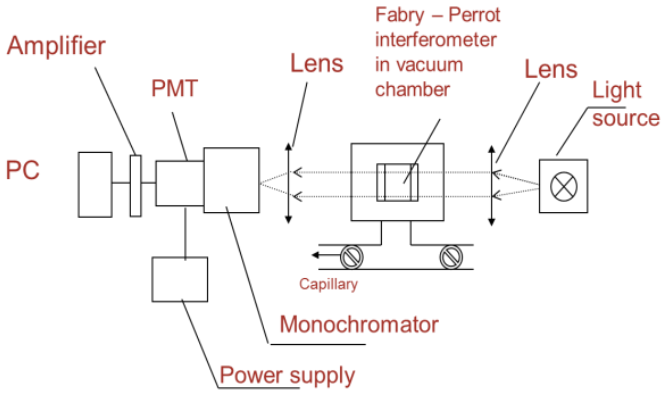

Figure 2. Set-up of a Fabry Perot high resolution spectrometer.

The finesse of the interferometer is restricted by the effective refraction coefficient of the mirrors which includes both, the refraction coefficient and inaccuracy of the adjustment. For example at the effective refraction coefficient R = 80%, the full width at half of maximum (FWHM) of the instrument function $\Delta\nu_{instr}$ amounts to 0.071 cm^{-1}.

2.2. Zeeman Spectrometer

Since The principle set-up of the scanning Zeeman spectrometer is shown in Fig. 3(a). This type of spectrometer is very useful to measure the resonance line shapes in UV region [3, 4]. Examples of the measured Hg VUV resonance line of 185 nm wavelength are shown in Fig.3 (b). By our knowledge this is the only available spectrometer which makes possible direct registration of the Hg 185 nm spectral line shape. The light from the plasma source traverses the same metal vapour cell. The frequency scanning is ensured by changing the magnetic field strength in the absorption cell. The signal is registered by the PMT.

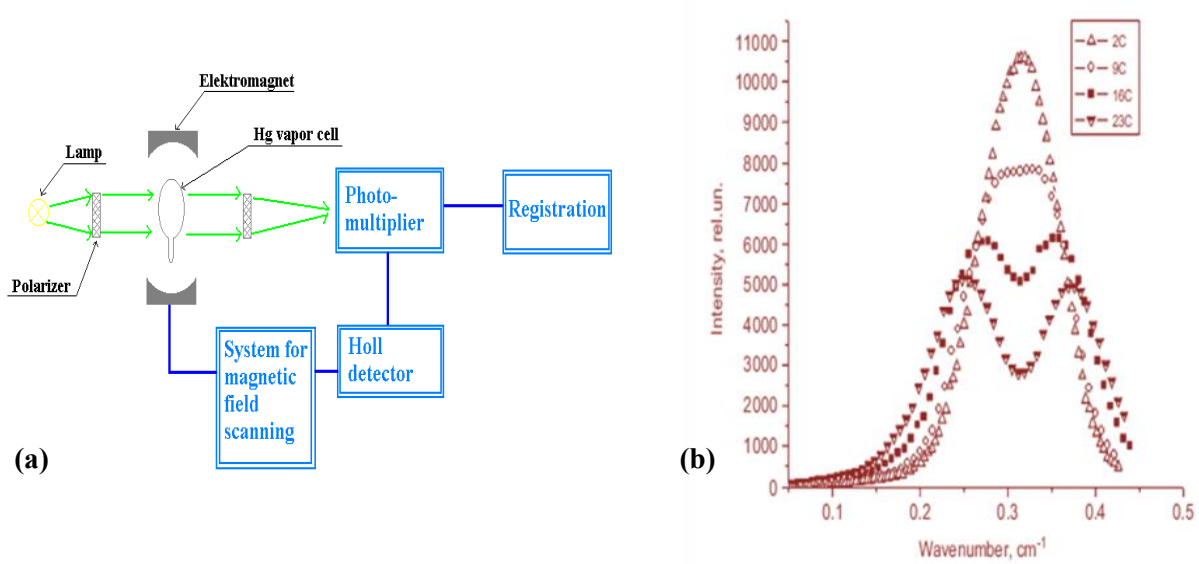

Figure 3. (a) Set-up of Zeeman high resolution spectrometer for the line shape measurements based on absorption of light in the cell placed in magnetic field; **(b)** experimentally measured Hg resonance line shape of 185 nm emitted from the Hg isotope 198 lamp in dependence of the Hg cold spot temperature (metal vapour pressure) [4].

For the Zeeman spectrometer, the instrument function is absorption profile of the metal vapor in the absorption cell. If the cell is hold at the room temperature of 20^{o} C, the Doppler broadened absorption profile has FWHM of 0.036 cm^{-1} which gives better resolution than for the Fabry-Perot interferometer.

2.3. Fourier Transform Spectrometer

The Fourier Transform Spectrometer model Bruker IFS 125 HR can be used to measure spectral line shapes in wide spectral range from 320 - 910 nm, about 2000 pixels/nm. The theoretical instrument function of the Fourier spectrometer is function sinc(x) = sin(x)/x shown in Fig.4. However the measured function using the He laser line of wavelength 632.8 nm, shown in Fig.5 looks differently.

Since the reconstruction takes into account the theoretical or measured prompt function and since we encountered issues with finding stable solutions, we first applied a fitting procedure. Subsequently, we found that the best approximation of the instrument function is a Lorentz profile with FWHM of 0.02 cm^{-1} [5]. Thus all further calculations were performed with this function. Experimentally measured spectral line shapes of 435.8 nm for two Hg isotope lamps, 202 and 198 isotopes, respectively, depend on the discharge power. Fig. 6 displays these results.

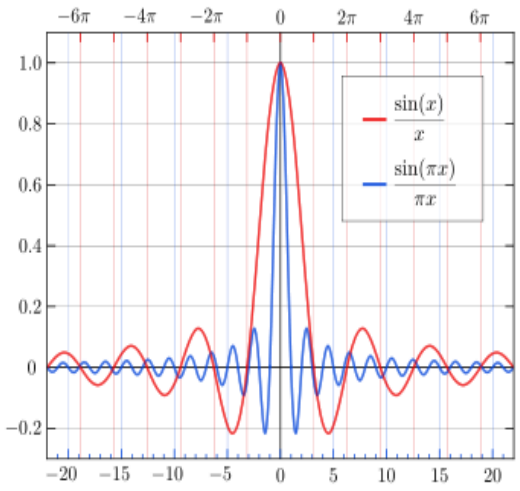

Figure 4. Theoretical instrument function of Fourier transforms spectrometer.

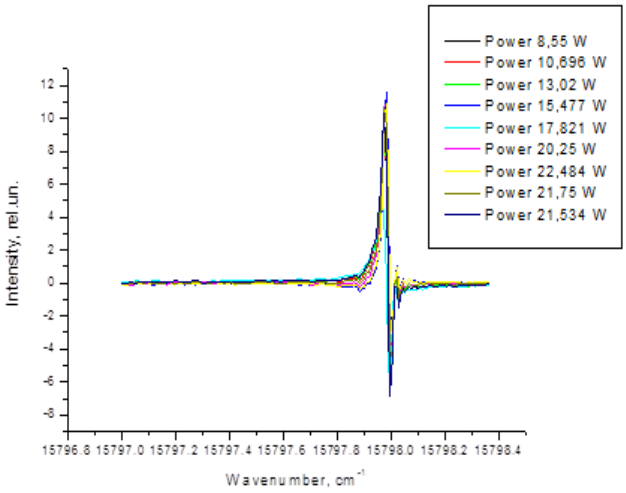

Figure 5. Experimentally measured Fourier transform spectrometer instrument function.

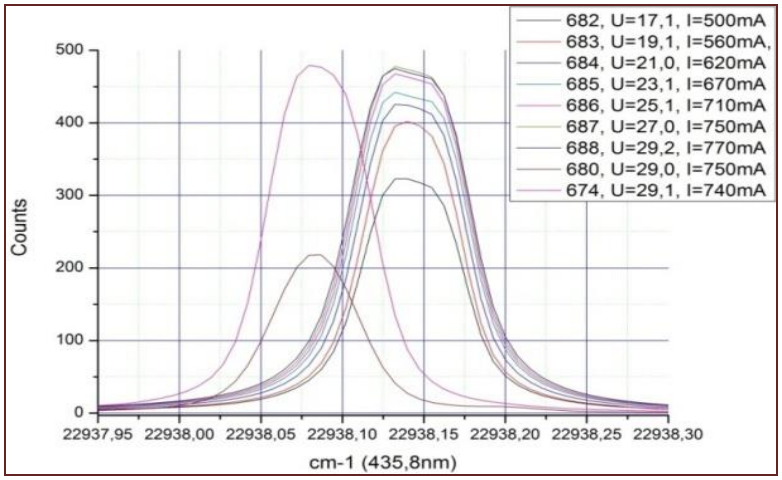

Figure 6. Experimentally measured Fourier spectra of the Hg 435.8 nm line shapes for the two Hg isotopes 198 and 202.

3. Theoretical Approach

As is well known, the experimentally registered spectral line shape, influenced by the instrument function, can be expressed in form of a Fredholm integral equation of first kind:

$$\int_a^b A(x,s)y(s)ds = f(x), \quad c \le x \le d, \quad (1)$$

where *f(x)*- measured spectral line profile; *y(s)*- real spectral line profile; *A(x,s)*-instrument function and a, b and c, d -the limits of the real and experimental profiles, accordingly.

To calculate the real spectral line profile from experimental line, it is necessary to solve this inverse ill-posed task where small experimental uncertainties can cause large deviations in the solution. Our experience showed that the Tikhonov's regularisation algorithm [6] is one of the most useful tools for solving the task.

Assuming, that the values on the right side and integral equation (1) kernel are known with accuracy:

$$\left.\begin{aligned} \left\| \tilde{f} - f \right\|_F \le \delta; \\ \left\| \tilde{A} - A \right\| \le \xi \end{aligned}\right\} \qquad (2)$$

where δ is the error of right part of (1) or the error of experimental $f(x)$ profile, ξ is the error of kernel of (1) or the error of instrument function $A(x,s)$, Tikhonov proved, that the initial, ill-posed task can be transformed into a task of searching for the minimum of a smoothing functional:

$$M_\alpha\left[y, \tilde{f}\right] = \inf_{y \in Y} M_\alpha\left[y, \tilde{f}\right], \qquad (3)$$

where the smoothing functional $M_\alpha\left[y, \tilde{f}\right]$, so called Tikhonov's functional, is given in the form:

$$M_\alpha\left[y, \tilde{f}\right] = \left\| \tilde{A}y - \tilde{f} \right\|_F^2 + \alpha\Omega[y]. \qquad (4)$$

The stabilising functional Ω is described by the following expression:

$$\Omega[y] = \|y\|_Y^2 \qquad (5)$$

$\alpha > 0$ is the regularisation's parameter; the number discrepancy is denoted by $\left\| \tilde{A}y - \tilde{f} \right\|_F^2$.

According to Tikhonov's method, instead of the initial ill posed problem (1) we get well posed task, which is described by the Fredholm integral equation of second kind. After changing the integrals to finite sums, one can write the system of linear equations are

$$\sum_{i=1}^{N} b_i \left(\sum_{m=1}^{N} b_m \tilde{A}_{mk} \tilde{A}_{mi} \right) y_i + \alpha y_k = \sum_{m=1}^{N} b_m \tilde{A}_{mk} \tilde{f}_m, \quad k = \overline{1, N} \qquad (6)$$

where A_{ij} – elements of *N xN* size matrix *A,* which approximates kernel; f_i – vectors-column with initial dates; y_i – vector-column of solution; b_i – the coefficients.

The system of Equations (6) can be solved with classical methods. All calculations in this work were done for zero order of regularization (q=0) using programs written in MathCad. Regularisation parameter α was obtained in supposition, that the error of kernel is equal to zero (ξ=0) in cases when the instrumental function is known analytically. Typically we use two independent methods to obtain the regularisation parameter α [7,8].

However the deconvoluted real spectral line shape still needs to be modelled because we want to obtain plasma parameters. In the low temperature plasma the real spectral line shape can be approximated Voigt profile which is a convolution of the Doppler and Lorentz profiles. Normally, the Doppler width (FWHM), $\delta\nu_D$, and Lorentz width, $\delta\nu_L$, are used as the parameters characterizing the Voigt profile. Voigt profile includes the basic factors causing the spectral line broadening in a low-pressure discharge: natural, temperature, collisional. The main problem is to take into account the self-absorption. Spectral line modelling is further described in [2-4]. Along the line of sight the intensity distribution in the line shape *I(ν)* can be written as:

$$I(\nu) = I_0 \int_{-\infty}^{+\infty} \bar{n}_e(r) P_e(\nu, r) \exp\left[-s \int_r^{\infty} P_a(\nu, x) \bar{n}_a(x) dx \right] dr \qquad (7),$$
$$\bar{n}_a(r) = \frac{n_a(r)}{N_a}; \quad \bar{n}_e = \frac{n_e(r)}{N_e}$$

where

$$N_a = \frac{1}{2} \int_{-\infty}^{+\infty} n_a(r) dr; \qquad N_e = \int_{-\infty}^{+\infty} n_e(r) dr \,.$$

It is important to know the distributions of the absorbing and emitting particles $n_a(r)$ and $n_e(r)$. For our calculations we use several approximations: uniform distribution of emitting and absorbing particles (homogenous light source), light source with spatially resolved emitting and absorbing particles (inhomogeneous light source), experimentally determined distributions as well as model supposed by Cowan and Dicke which gives some kind of intermediate distributions of the excitation function of the light source [9].

4. Results and discussion

Mercury 202 isotope 253.7 nm line shapes, recorded with a Zeeman spectrometer and the Fabry-Perot spectrometer are shown in Fig. 7.

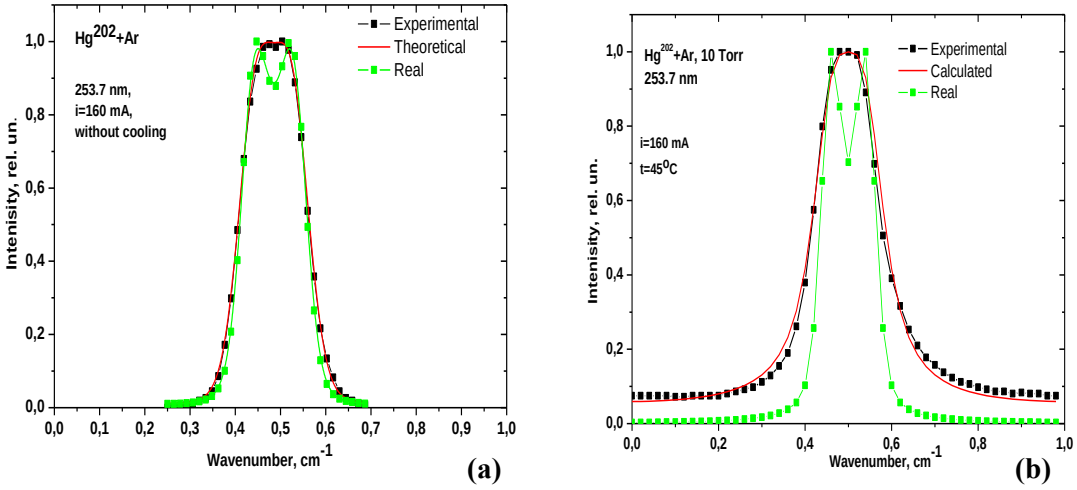

Figure 7. Comparison of mercury 202 isotope 253,7 nm line shapes, registered with Zeeman **(a)** and Fabry-Perot spectrometers **(b)** and the calculated real spectral line (green squares).

As we can observe, in both cases the dip due to the self-absorption is covered by the instrument functions of the spectrometers despite the fact that the instrument functions in both cases are narrow (the broadening is on the same order as the line shape itself). The Fabry-Perot spectrometer gives more influence on the wings of the shape. For the calculation of the real profile, the model of the inhomogeneous light source excitation function was applied. In Fig. 8, the results of deconvolution procedure are shown for Hg 546.1 nm visible triplet line.

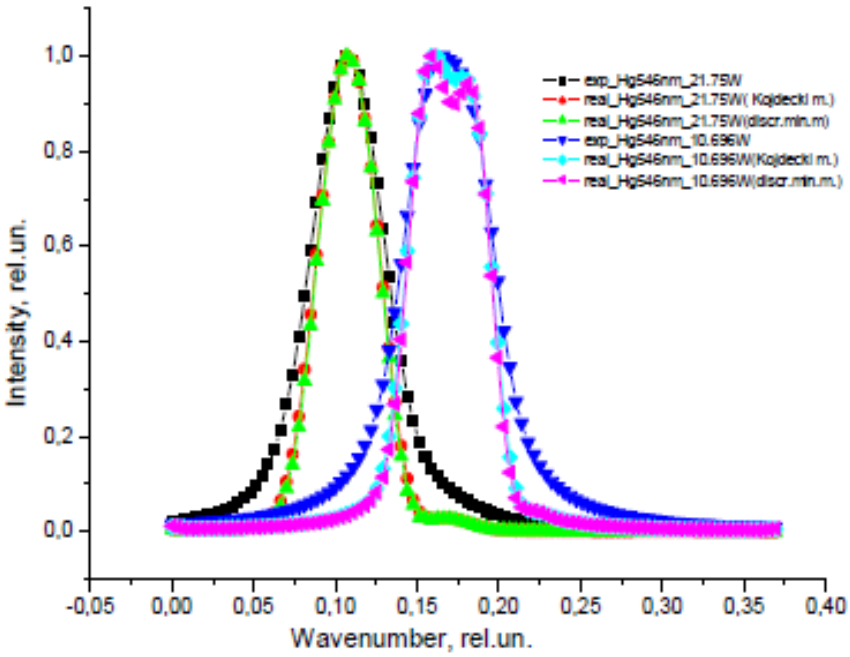

Figure 8. Experimental Fourier spectra of the Hg 546.1 nm line and deconvoluted shapes for the two Hg isotope lamps, 202 and 198.

The results are given for two methods of finding the regularization parameter α, the Kojdecki method [7] and minimum of discrepancy method [8]. Both methods give similar results. It is interesting to observe that the line, emitted from the 198 isotope lamp, is self-absorbed because the lamp contains higher concentration of mercury.

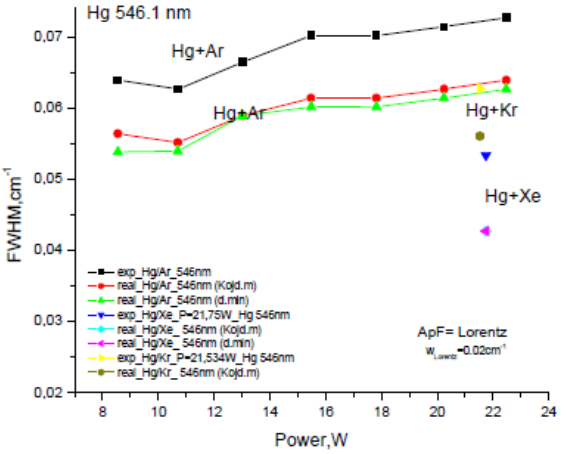

Figure 9. FWHM in dependence from the discharge power, calculated from the deconvoluted line shapes of Hg line 546.1 nm emitted from the Hg/Ar, Hg/Kr, Hg/Xe discharge plasmas.

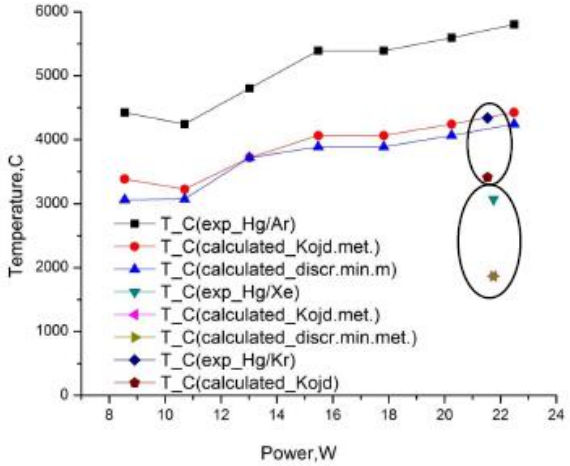

Figure 10. FWHM in dependence from the discharge power, calculated from the deconvoluted line shapes of 435.8 nm Hg line emitted from the Hg/Ar, Hg/Kr, Hg/Xe discharge plasmas.

We can obtain the real FWHM for all the registered lines that allows us to determine temperature of the emitting particles. Examples of the results of the calculated FWHM of the 546.1 nm line and temperatures (T) are shown in the Figs. 9 and 9. It is clearly demonstrated that the neglecting instrument function can lead to large error of about 1500° C in the temperature calculations. Clear

dependence of the temperature of the type of buffer gas can be observed – the heavier the buffer gas, the colder the plasma. Adding Kr instead of Ar decreases temperature of about 900^{o} C, adding Xe instead of Ar decreases temperature about 2000^{o} C.

5. Conclusion

Narrow spectral line shapes, emitted from the light sources, developed for the atomic absorption spectrometry for detection of heavy metals and benzene, are analysed by three different measurement methods in UV and visible spectral regions. The regularisation method and mathematical modelling is used to extract the real spectral line shape. Neglecting the instruments function gives an error of about 1500^{o} C for the discharge temperature. Clear influence of buffer gas type was found on the mercury discharge temperature.

Acknowledgement

This research has been partly supported by the European Social Fund within the project "Elaboration of Innovative Functional Materials and Nanomaterials for Application in Environment Control Technologies" 1DP/1.1.1.2.0/13/APIA/VIAA/30.

References

[1] Ganeev A, Gavare Z, Khutorshikov V I, Khutorchikov S V,Revalde G, Skudra A, Smirnova GM, Stankov N R 2003 *Spectrochim. Acta Part B* **58** 879
[2] Skudra A, Revalde G 1999 *J. Quant. Spectrosc. Rad. Transfer* **61** 717
[3] Revalde G, Denisova N, Gavare Z, Skudra A 2005 *J. Quant. Spectrosc. Rad. Transfer* **94** 311
[4] Revalde G, Skudra A, Zorina N, Sholupov S 2007 *J. Quant. Spectrosc. Rad. Transfer* **107** 164
[5] Revalde G, Zorina N, Skudra A, Gavare Z 2014 *Romanian Reports in Physics* **66** (in press: *N4*)
[6] Tikhonov A, Arsenin V 1979 *The solution's methods of the ill-posed problem* (Moscow: Nauka)
[7] Verlan F, Sizikov V S 1986 The integral equations: the methods, algorithms, program (Kiev: Naukova Dumka)
[8] Kojdecki M F 2000 New criterion of regularization parameter choice in Tikhonov's method *Biuletyn WAT* (Biul. Mil. Univ. Technol.) **49** № 1 (569) 47
[9] Cowan R D, Dieke G H 1948 *Rev. Mod. Phys*. **2** 418